

Structural and optical properties of TiO₂ :C (Titanium dioxide with Carbon) nanocrystals for Photoluminescence devices

K. Gayathiridevi , Department of Physics, Bharathidasan University Constituent College for Women, Orathanadu, India, swasthikadevi12@gmail.com

G. Pasupathi * , Department of Physics, A.V.V.M. Sripushpam College (Auto), Poondi, India, aamariam786@gmail.com/ gpasupathi123@gmail.com

Abstract: The vibrational groups of the TiO₂:C single crystal have been investigated by FTIR, Laser- Raman analyses. It has low absorbance in the UV-Vis-NIR region. The band gap of the material is calculated as 3.42 eV. The optical studies were carried out at the frequency regions and band gap value is plotted with respect to the wavelength 300 – 900 nm. Non-linear optical nanocrystal TiO₂:C has been grown by hydrothermal technique. Its transmission is very high (80%) as a transparent materials reported here, low absorbance value was measured because of its nanosize. The fingerprint plots contain the highest portion of O - H and C interactions. The morphological studies were analyzed by using Scanning Electron Microscopy with EDAX analysis to confirm the materials prepared by the hydrothermal technique.

Keywords — TiO₂:C, UV-Vis spectroscopy, Fourier Transform Spectroscopy, Photoluminescence, Emission and Nanocrystals

I. INTRODUCTION

Different optoelectronic and electrical materials have motivated researchers to grow semi-organic single crystals for advanced high technology devices. Carbon materials are having nonlinear optical properties have evolved as one of the important field of research for various applications such as communication, optical electronics, optical data storage, laser frequency shifting, optical limiting, and optical data processing and so on. The carbon structured crystals are combining the advantages of both organic and inorganic materials which have high thermal stability, large transmittance range, mechanical strength and so on [1, 2]. TiO₂ with Carbon is one of the single crystals and crystallizes in triclinic crystal system with the space group P1. Due to these promising properties, TiO₂ with its composites crystal makes it a good candidate for image processing and so on [3]. Titanium with metal has asymmetric hydrogen bond chains along [101] plane [4], the TiO₂ with Carbon bonding materials has promising piezoelectrics and NLO properties [5]. The photoinduced absorption is one of the important factors for increasing second and third order nonlinear optical susceptibility. This originates from the photoinduced electron phonon and harmonicities [6]. Crystal growth is a non-equilibrium process and thus prone to defects incorporation during growth. Defects can be classified as point defects, linear

defects, planar defects and volume defects. All these defects influence the quality of the crystal. Hence, evaluating defects provides elaborate information about the crystal quality and functional characteristics of the crystal. Analysis of defects in the crystals is crucial because present and future applications demand defects free single crystals [7].

Nucleation kinetics, crystal perfection, transmittance, photoconductivity properties of TiO₂:C nanocrystal [8], by hydrothermal growth technique and their intermolecular interactions, FT-Raman, optical band gap and morphological properties.

II. EXPERIMENTAL ANALYSIS

The presence of Titanium in well known optical crystals, Titanium carbide (TiC) 99%, Graphite flakes 1 %, and Glycene 0.5% and 1% Na₂HPO₄.12H₂O, NH₄Cl, Graphite flakes (C), TiC and Sodium citrate were purchased from Sigma Aldrich Chemical Reagent (Ltd) 99% purity. Also such a metal organic compound is expected to combine superior physical properties of their counterparts. This combination was diluted in the 100 mL solution and it was stirred for 3 hrs by using magnetic stirrer. Then the solution was stored in autoclave at constant temperature bath at 160 °C at pressure of 15 atmospheres. Optically clear and well-shaped crystals suitable for usage as seed crystals were obtained in the course of 7 days. Very small TiO₂:C nanocrystals were grown in a crystallizer using

hydrothermal growth method. Transparent crystals of size: $1.0 \times 1.0 \times 1.0 \text{ mm}^3$ were obtained in a period of about 7 days [9].

III. RESULTS AND DISCUSSION

Figure 1 shows the XRD pattern of the $\text{TiO}_2\text{:C}$ sample by hydrothermal technique on can be seen that the $\text{TiO}_2\text{:C}$ sample are broad peak appearing at low angle is much less due to the fact that the $\text{TiO}_2\text{:C}$ sample are strong crystalline at the predominant peak and mostly for the amorphous nature due to the nanosize. The structure changes from amorphous to crystalline. sample are better and only one strong peaks are observed is due to the orientation is enhanced for phase formation under the influence of hydrothermal method. This is actually due to the increase in the intensity (counts) of the peaks. Structural geometry of $\text{TiO}_2\text{:C}$ nanocrystals is having tetragonal structure and its lattice variations are shown in Figure 2(a-b). For the tetragonal system the interplanar distances are calculated by

$$\text{using the equation } \frac{1}{d^2} = \frac{(h^2 + k^2)}{a^2} + \frac{l^2}{c^2}$$

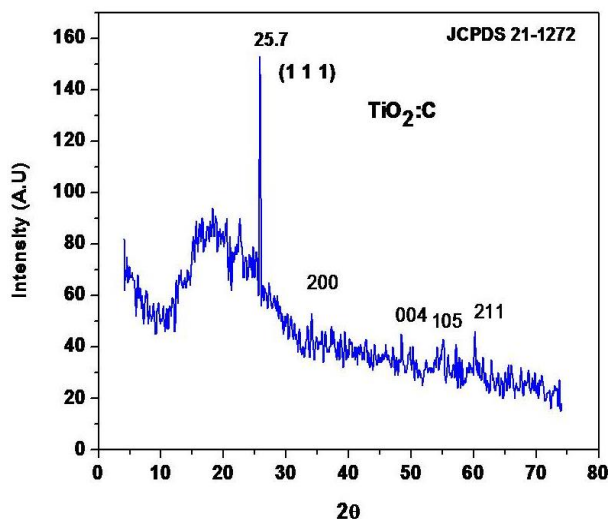


Figure 1 XRD Analysis of $\text{TiO}_2\text{-C}$ nanocrystals

However, no phase change is observed in the sample in Figure 2 intensity the prominent peak (101) is improved significantly and also all other subsidiary peaks are prominent. In the as-deposited film only the (101) peak is prominent. All other peaks (200), (004), (105) and (211) are not intense well matched with JCPDS file 21-1272 and it is agreement with refinement analysis shown in Figure 2 [10].

The crystal size of the predominant plane by using its FWHM was calculated by the equation $D = \frac{0.94\lambda}{\beta \cos\theta}$

Table-1 Structural Studies of $\text{TiO}_2\text{:C}$ nanocrystals

| Sample | Crystal Size (nm) | hkl | Lattice constant A° | |
|---------------------------------------|-------------------|-----|---------------------|-----------|
| | | | a | c |
| $\text{TiO}_2\text{:C}$ Tetragonal | 45 | 101 | a = 3.785 | c = 9.513 |
| | | 101 | 3.779 | 9.492 |

Predominant planes presented in this spectrum have higher intensities than those observed for the sample, which could be associated with a grain growth effect shown by the geometry of the $\text{TiO}_2\text{:C}$ crystal shown in Figure 3(a-b). The peaks related with tetragonal phase are observed and it was reported here.

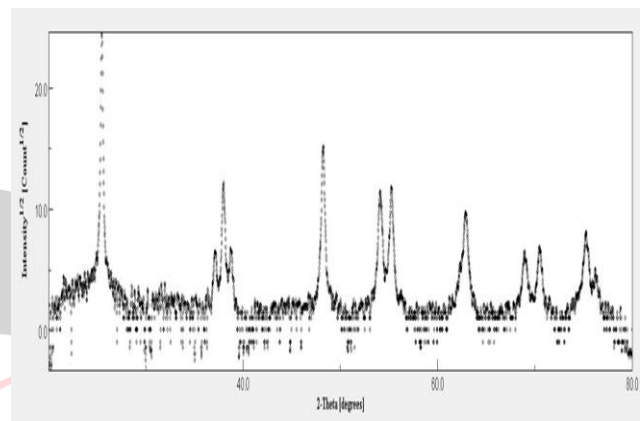


Figure 2 Reitveld refinement of $\text{TiO}_2\text{:C}$ nanocrystals of XRD Analysis

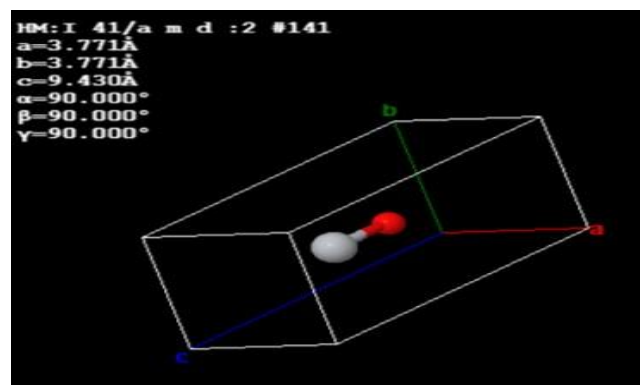
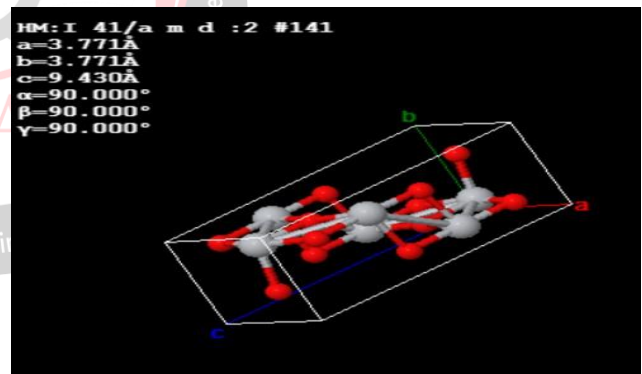


Figure 3 (a-b) Structural geometry of $\text{TiO}_2\text{:C}$ crystals

SEM Analysis

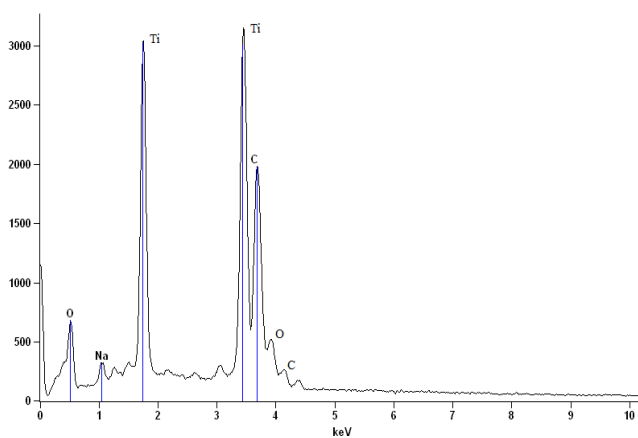
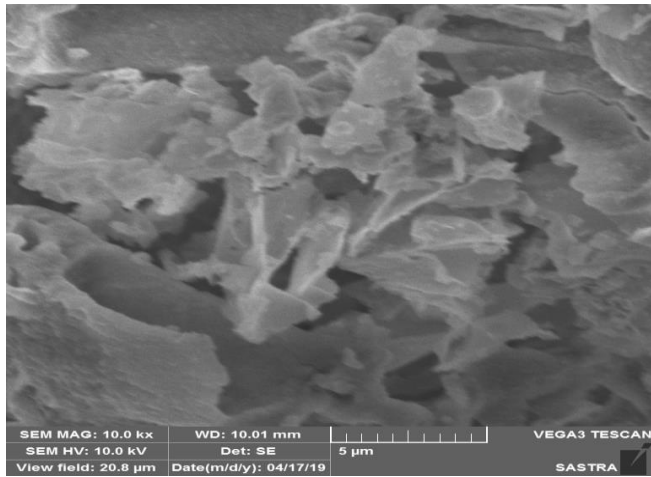


Figure 4(a-b) SEM with EDAX Analysis of TiO₂:C nanocrystals

Table -2 EDAX Analysis of TiO₂:C nanocrystals

| Element | Net Counts | Weight % | Atom % |
|--------------|------------|----------|--------|
| O | 4432 | 21.86 | 53.41 |
| Na | 1425 | 2.22 | 3.78 |
| Ti | 31717 | 14.85 | 20.68 |
| C | 6151 | 3.13 | 3.05 |
| Ti | 71167 | 57.94 | 19.09 |
| Total | | 100.00 | 100.00 |

SEM image is giving a good morphological impression of the sample and its micrographs of the TiO₂:C crystals is shown in Figure 4a. These platelets are clustered forming large grains of up to many thousand μm diameter. It may further follow that such grains reach from the top surface of the electrode to the backplane. This would lead to unhindered charge transfer across the crystal, resulting in the good structural behavior. This may be the reason to have high crystallinity in the prepared nanocrystals of TiO₂: C due to the conversion of grains into platelets [11]. Table 2 shows the proportions of the compounds Ti, O and C compositions and its percentage present inside the

nanoparticles. The EDAX elemental analysis of TiO₂:C is shown in Figure 4b.

FTIR Analysis

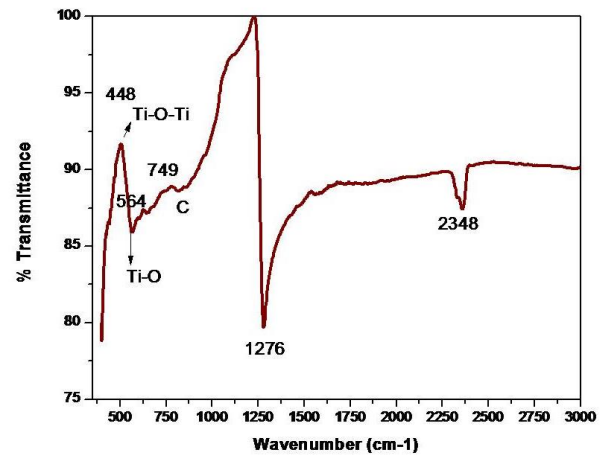


Figure 5 FTIR Study of TiO₂:C crystals

The FTIR transmission spectra of TiO₂:C are shown in Figure 5. The FTIR spectrum of the sample comprises transmittance bands at 448 cm⁻¹, 564 cm⁻¹, 749 cm⁻¹, 1276 cm⁻¹ and 2348 cm⁻¹. The sharp peaks appearing at 448 cm⁻¹ and 749 cm⁻¹ are associated with the longitudinal and transverse optical phonon modes respectively for TiO₂:C [12]. The peaks at 564 cm⁻¹ and 1276 cm⁻¹ are characterized as the vibration absorption of the Ti-O-C bond [13]. The band 2348 cm⁻¹ can be assigned to Sodium (Na) ions retained as impurity. These results reveal the fact that the increased intensity of these peaks confirms the formation of more stoichiometric TiO₂:C doping.

UV Vis NIR spectroscopy

The optical properties (transmittance and absorbance spectrum) of the TiO₂:C sample were studied by UV-Vis double beam spectrophotometer in the range of 300-900 nm. The plots of optical absorption versus wavelength spectra of TiO₂:C sample shows good absorption in the visible region of 300 – 900 nm. The absorption of TiO₂:C sample showed the sharp absorption peak are about 340-360 nm, which indicates a narrow size distribution of the product. The increase in absorption is due to the change in particle size. In this investigation transmission spectra of TiO₂:C sample have been recorded a gradual decrease in transmission starting from the wavelength region corresponding to the absorption edge of the TiO₂:C sample [14].

The as-deposited films were half-transparent over the wavelength range shown here. After annealing, the results showed that the absorbance edge is clearly observed and the absorbance edge is shifts towards lower energy than that of the TiO₂:C sample. This is probably due to increase in the grain size. The shift indicates increase in band gap of the sample. The optical transmittance of the TiO₂:C sample,

show an over 80% in the visible region, shows very weak transparency below 69% in the visible light range.

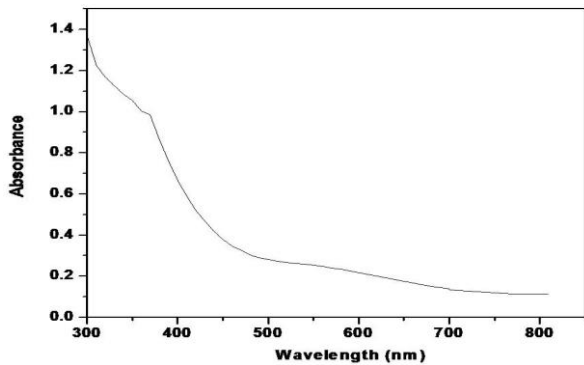


Figure 6a Absorbance of TiO₂:C nanocrystals

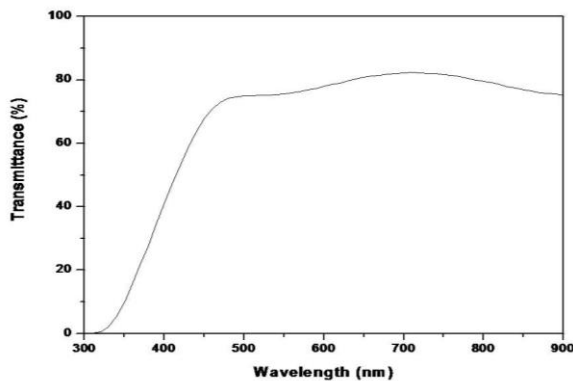


Figure 6b Transmittance of TiO₂:C nanocrystals

TiO₂:C nanocrystals are having direct band gap was determined with the help of absorbance spectra. Figure 5c shows the band gap of TiO₂:C nanocrystals. Hence a plot of graph between $(\alpha h\nu)^2$ versus $h\nu$ of TiO₂:C given a straight line portion and extrapolated to cut the x-axis which gives the band gap. It was found to be 3.41 eV for the band gap results are increases and it can be attributed to the decrease in particle size and basic properties of these compounds. The band gaps values of TiO₂:C nanocrystals, which are considered to be optimum values for their use in high efficient optoelectronic devices [15].

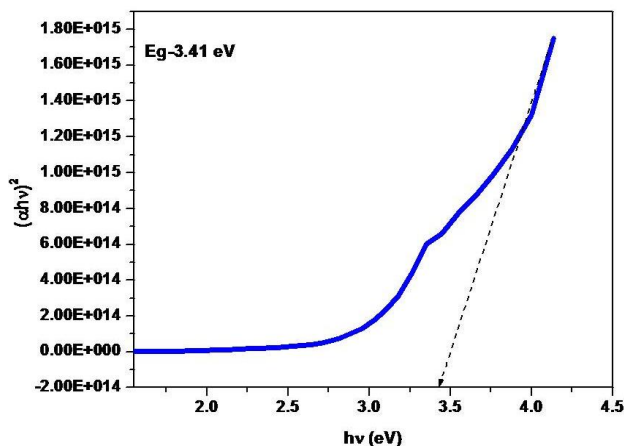


Figure 6c Bandgap analysis of TiO₂:C nanocrystals

Photoluminescence Analysis

The PL spectra of TiO₂:C for the as-prepared powder is shown in Figure 7, the PL spectrum mainly consists of sharp and broad emission band was a superimposition of two bands, which peaks at approximately 445 nm in blue region and a weak shoulder at around 700 nm in red region. The blue emissions may originate from the defects in TiO₂. It can be seen, the relative intensity of blue and red peak was linearly proportional to the doping of carbon dependent and the crystallinity of the TiO₂:C is improved with as-prepared powder [16].

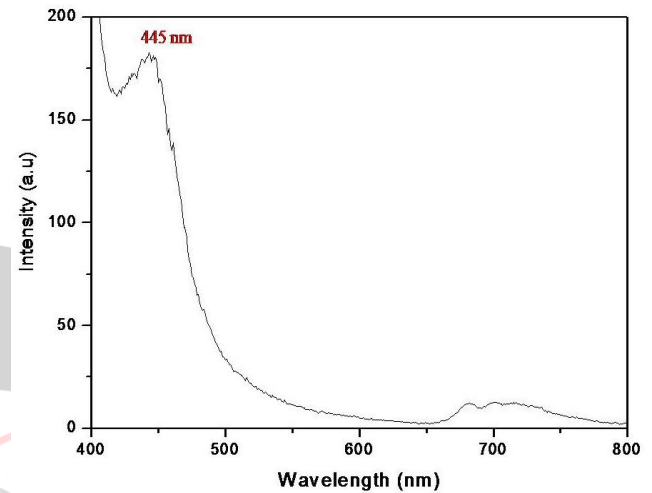


Figure 7 Photoluminescence Study of TiO₂:C crystals

Photoluminescence devices

Luminescence denotes the absorption of energy in matter and its reemission as visible or near visible radiation. Photoluminescence depends on excitation by electromagnetic radiation. The structural and optical properties are analyzed which have direct influence on the luminescent properties of TiO₂:C nanocrystals. The blue emission around 333 nm observed for this crystal when the excitation wavelength is 224 nm shown in Figure 8.

Blue shift in the absorption spectra was observed and its surface effect of exposing with UV light is shown in Figure 9 and its band gap and wavelength are listed in Table 3. The bright violet blue color of the powder after exposing UV light shows that this powder can be used in the development of efficient luminescent devices, so this powder prepared here will helpful in the production of low-cost luminescent devices.

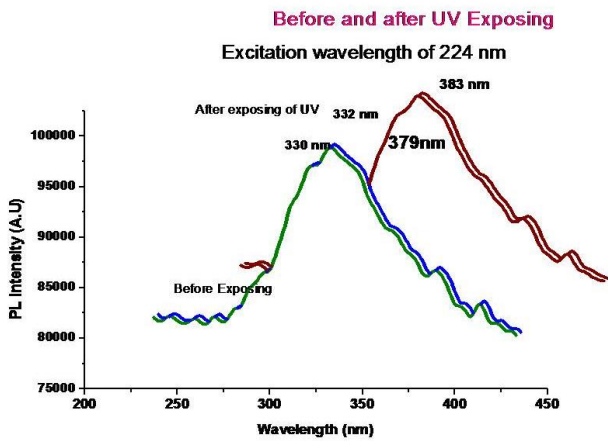


Figure 8 Photoluminescence emission spectra of TiO₂:C nanocrystals when the excitation is 224 nm

The excitation wavelength was 224 nm and the peaks are recorded at 333 nm which the emission band has high intensity can be attributed of impurity giving rise to violet-blue color luminescence. This may be due to the recombination of free charge carriers at defect sites, possibility at the surface of TiO₂:C nanocrystals [17].

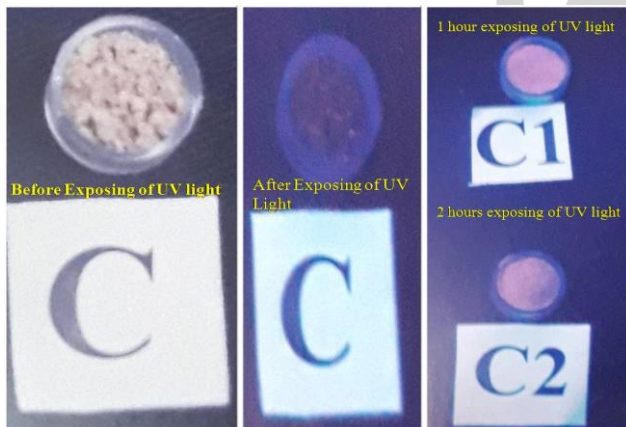


Figure 9 Photograph pictures of the TiO₂:C nanocrystals before and after exposing of UV light.

Table 3. Wavelength and Energy gap Before and after exposing of UV light radiation of TiO₂:C nanocrystals

| Before UV light Exposing | After UV light Exposing | | |
|--------------------------|-------------------------|------------|-------------|
| | Starting | After 1 hr | After 2 hrs |
| 330 nm | 332 nm | 379 nm | 383 nm |
| 3.709 eV | 3.686 eV | 3.229 eV | 3.195 eV |

IV. CONCLUSION

The prepared TiO₂:C nanocrystals are having crystal size of 45 nm and its excitation wavelength of before and after UV light exposing proved that it may act as a very cheap photoluminescence devices. The morphological studies explained the agglomeration of the particle with platelets structure in micrometer range. The vibrational spectrum of FTIR analysis explains the symmetric longitudinal and

optical absorption spectrum of the sample. The UV-Vis studies gave the band gap in direct allowed transition nearly equal to 3.41 eV.

REFERENCES

- [1]. G. Prabhavathi, A. Mohamed Saleem, A. Ayeshamariam*, N.Punithevelan, M. P. Srinivasan, and M. Jayachandran, Fabrication and Characterization of TiO₂:rGO Thin Films on Si Substrate by Spin coating technique for the Determination of Sensitivity of Methanol Gas Concentration”, International Journal for Research in Engineering Application & Management (IJREAM) ISSN : 2454-9150 Vol-04, Issue-10, Jan 2019
- [2]. Shao, J., Sheng, W., Wang, M., Li, S., Chen, J., Zhang, Y. and Cao, S., In situ synthesis of carbon-doped TiO₂ single-crystal nanorods with a remarkably photocatalytic efficiency. *Applied Catalysis B: Environmental*, 209, pp.311-319, 2017.
- [3]. Chen, D., Jiang, Z., Geng, J., Wang, Q. and Yang, D., Carbon and nitrogen co-doped TiO₂ with enhanced visible-light photocatalytic activity. *Industrial & engineering chemistry research*, 46(9), pp.2741-2746, 2007.
- [4]. Wang, H., Wu, Z. and Liu, Y., A simple two-step template approach for preparing carbon-doped mesoporous TiO₂ hollow microspheres. *The Journal of Physical Chemistry C*, 113(30), pp.13317-13324, 2009.
- [5]. Cong, Y., Li, X., Qin, Y., Dong, Z., Yuan, G., Cui, Z. and Lai, X., Carbon-doped TiO₂ coating on multiwalled carbon nanotubes with higher visible light photocatalytic activity. *Applied Catalysis B: Environmental*, 107(1-2), pp.128-134, 2011.
- [6]. Ren, W., Ai, Z., Jia, F., Zhang, L., Fan, X. and Zou, Z., Low temperature preparation and visible light photocatalytic activity of mesoporous carbon-doped crystalline TiO₂. *Applied Catalysis B: Environmental*, 69(3-4), pp.138-144, 2007.
- [7]. Zhou, B., Schulz, M., Lin, H.Y., Shah, S.I., Qu, J. and Huang, C.P., Photoelectrochemical generation of hydrogen over carbon-doped TiO₂ photoanode. *Applied Catalysis B: Environmental*, 92(1-2), pp.41-49, 2009.
- [8]. Qi, D., Xing, M. and Zhang, J., Hydrophobic carbon-doped TiO₂/MCF-F composite as a high performance photocatalyst. *The Journal of Physical Chemistry C*, 118(14), pp.7329-7336, 2014.
- [9]. Wu, Z., Dong, F., Zhao, W., Wang, H., Liu, Y. and Guan, B., The fabrication and characterization of novel carbon doped TiO₂ nanotubes, nanowires and nanorods with high visible light photocatalytic activity. *Nanotechnology*, 20(23), p.235701, 2009.

[10]. Kaviyarasu, K., Mariappan, A., Neyvasagam, K., Ayeshamariam, A., Pandi, P., Palanichamy, R.R., Gopinathan, C., Mola, G.T. and Maaza, M., Photocatalytic performance and antimicrobial activities of HAp-TiO₂ nanocomposite thin films by sol-gel method. *Surfaces and Interfaces*, 6, pp.247-255, 2017.

[11]. Tang, H., Berger, H., Schmid, P.E., Levy, F. and Burri, G., Photoluminescence in TiO₂ anatase single crystals. *Solid State Communications*, 87(9), pp.847-850, 1993.

[12]. Ong, W.J., Tan, L.L., Chai, S.P., Yong, S.T. and Mohamed, A.R., Self-assembly of nitrogen-doped TiO₂ with exposed {001} facets on a graphene scaffold as photo-active hybrid nanostructures for reduction of carbon dioxide to methane. *Nano Research*, 7(10), pp.1528-1547, 2014.

[13]. Mao, C., Zuo, F., Hou, Y., Bu, X. and Feng, P., In situ preparation of a Ti³⁺ self-doped TiO₂ film with enhanced activity as photoanode by N₂H₄ reduction. *Angewandte Chemie International Edition*, 53(39), pp.10485-10489, 2014.

[14]. Zhou, H. and Zhang, Y., Electrochemically self-doped TiO₂ nanotube arrays for supercapacitors. *The Journal of Physical Chemistry C*, 118(11), pp.5626-5636, 2014.

[15]. Zhang, Z., Yang, X., Hedhili, M.N., Ahmed, E., Shi, L. and Wang, P., Microwave-assisted self-doping of TiO₂ photonic crystals for efficient photoelectrochemical water splitting. *ACS applied materials & interfaces*, 6(1), pp.691-696, 2013.

[16]. Nah, Y.C., Paramasivam, I. and Schmuki, P., Doped TiO₂ and TiO₂ nanotubes: synthesis and applications. *ChemPhysChem*, 11(13), pp.2698-2713, 2010.

[17]. Zaleska, A., Doped-TiO₂: a review. *Recent patents on engineering*, 2(3), pp.157-164, 2008.